From the Department for Companion Animals and Horses
of the University of Veterinary Medicine Vienna

Division of Small Animal Internal Medicine
(Head: Univ.-Prof. Dr.med.vet. Iwan A. Burgener, PhD, Dipl.ECVIM-CA Dipl.ACVIM)

Identification of canine melanoma cancer stem cells

Bachelor thesis

University of Veterinary Medicine Vienna

Philipp Georg Schmelz

Vienna, June 2022

Supervisor: Mag[a] rer.nat. Dr[in] rer.nat. Barbara Pratscher

Reviewer: Dipl.-Ing[in] Dr[in] nat.techn. Priv.-Doz[in] Sabine Brandt

Acknowledgements

I would like to thank Prof. Iwan A. Burgener and the whole Division of Small Animal Internal Medicine team for the warm welcoming and giving me the opportunity to work there on my bachelor thesis.

Special thanks go to Dr. Barbara Pratscher for her support and help through the entire writing and practical process.

Further thanks go to Susann Schönefeldt for her expertise in flow cytometry she shared with me, and to the whole team of the VetBiobank, especially Stefan Kummer, for introducing and explaining me all the immunostaining methods and fluorescence microscopy.

Last but not least, I would like to thank my family for supporting and encouraging me along my way.

Table of contents

1. Introduction

1.1. General background

Canine oral malignant melanoma (cOMM) has a high metastatic potential and is a relatively common tumour disease in dogs. Malignant tumour lesions are generally characterized according to the TNM classification system. “T” stands for “Tumour” and describes the size of the primary tumour and its ability to invade neighbouring tissues. “N” is the abbreviation for “Nodes” describing the involvement of regional lymph nodes in tumour spread. “M” stands for “Metastasis”, specifying whether more distant spread beyond regional lymph nodes occurs. With respect to these tumour properties, four stages can be distinguished with stage IV describing metastatic cancer (Rosen & Sapra, 2022).

COMM is categorized into four stages. Stage I refers to tumours < 2 cm in diameter, stage II to tumours 2 to 4 cm in diameter, stage III to lesions > 4 cm in diameter and/or lymph node metastasis, and stage IV to distant metastases (Bergman, 2007). Since dogs are companion animals living in very close contact with humans and share the same environment including possible carcinogens, cOMM represent a valuable model for human malignant melanoma (hMM). This is even more so since cOMM and hMM are also similar with respect to the biological mechanisms underlying tumour development and progression (Atherton et al., 2016). Moreover, besides surgical interventions and chemotherapy there are also a few promising immunotherapy possibilities for cOMM (Almela & Ansón, 2019).

A major reason for the tumour cells’ resistance against cancer treatments is their plasticity. Cell plasticity is the ability to switch from one phenotype to another due to environmental changes. It allows stem cells to differentiate into progenitor cells of another tissue, like bone marrow cells becoming cardiomyocytes, and it helps the cancer cell to evade the immune system and acquire multidrug resistance (MDR) (Boumahdi & de Sauvage, 2019; Yoder, 2004). Another prominent example where this phenotype switching occurs, is epithelial-mesenchymal transition (EMT), which is recognized as a critical process during embryonic development and wound healing, but also cancer invasion and metastasis (Mani et al., 2008; Yang & Weinberg, 2008).

During EMT, epithelial cells lose their typical properties including cell-cell-adhesion, apical-basolateral polarisation and morphology, and gain mesenchymal characteristics such as enhanced migratory capacity, invasiveness and resistance to apoptosis promoting metastasis (Cervantes-Arias et al., 2013; Kalluri & Weinberg, 2009; Strohmayer et al., 2022). The reverse process of EMT is mesenchymal-epithelial transition (MET), causing repolarisation and organisation of the epithelium by re-creating inter- and extracellular interactions, including rebuilding of cell-cell junctions (Pei et al., 2019).

In the past years, it has been shown that EMT is also associated with a gain of cancer stem cell (-like) (CSC) properties (Dongre & Weinberg, 2018; Mani et al., 2008). An important feature shared by normal stem cells and CSCs is the ability for self-renewal and differentiation into multiple cell types, leading to the creation of heterogenous cell population within the tumour. For this reason, CSCs are also referred to as tumour- initiating cells (Nimmakayala et al., 2019; Reya et al., 2001).

Importantly, phenotype switching to CSCs is reversible. Due to their high plasticity, cancer cells can change between a CSC and a non-CSC state, making stemness a dynamic property (Thankamony et al., 2020). Furthermore, CSCs are quiescent cells that resist to various stress factors, such as DNA damage, reactive oxygen species, drug application and chemo- or radiation therapy (Diehn et al., 2009; Nimmakayala et al., 2019; Vitale et al., 2017).

1.2. Biomarkers

In cOMM, only scarce information is available on the presence and pathogenic role of CSCs. Nevertheless, there are a several potential cluster of differentiations (CD) markers for CSCs in general, and specifically in connection with melanoma. In this thesis, two of these potential CD markers will be investigated for cOMM.

The first is CD44, a transmembrane glycoprotein described as a reliable general marker for CSCs (Morath et al., 2016). Quintana and her colleagues showed that murine immunosuppression levels have a significant impact on the carcinogenicity of transplanted human melanoma cells. Notably Interleukin-2 receptor deficient SCID mice were highly permissive for invasive growth and metastasis of human patient-derived melanoma cells irrespective of CD44 expression by these cells (Quintana et al., 2008). This finding can be

explained by the relatively high artificiality of this xenotransplantation approach. Moreover, CD44 is a multifunctional receptor that binds not only to hyaluronic acid but also to other extracellular matrix (ECM) components such as collagen, fibronectin, or laminin (Naor et al., 1997). In addition, several of its ligands are growth factors and cytokines regulating gene expression, so that CD44 has a key role in cell-cell and cell-ECM interactions, cell differentiation and proliferation, and thus also in tumour initiation (Elkashty et al., 2020; Yan et al., 2015). In addition, CD44-positive cells are more resistant to radiation and show an increased probability to metastasize to regional lymph nodes (Chinn et al., 2015; Diehn et al., 2009). These features are typical for CSCs.

Another important marker for malignant melanoma is the nerve growth factor receptor CD271. It is known that epithelial cells express CD271, and that this marker is associated with perineural invasion in malignant melanoma. Therefore, CD271 is assumed to have a potential role in metastasis, notably in relation with the nervous system and brain (Chan & Tahan, 2010; Civenni et al., 2011; Davies et al., 1987).

Boiko and his colleagues were the first to propose a crucial role of CD271 in melanoma development. The group showed that transplantation of human CD271-positive melanoma cells, but not CD271-negative cell equivalents resulted in tumour development and metastasis in mice (Boiko et al., 2010). Furthermore, there is evidence of CD271-positive cells representing a subpopulation within the CD44-positive cell fraction in squamous cell carcinoma of the head and neck. Cells positive for CD44 and CD271 demonstrate higher cell proliferation rates, increased resistance to chemo- and radiotherapy as well as sphere formation compared to CD44-positive CD271-negative tumour cells (Elkashty et al., 2020; Murillo-Sauca et al., 2014).

These findings support the concept that CD271 might be the determining factor within the CD44-positive cell compartment in the formation of melanoma. However, it has been shown that CD44-negative cells can initiate tumours and contribute to MDR as well, making it necessary to assess expression of both markers on tumour cells (Oh et al., 2013).

1.3. Methods background

Cell culture is a basic method for investigating the properties of cells. Primary cells, which are “finite” cells directly explanted from tissues, transformed cells, naturally or modified

“immortalized” cells such as cancer cell lines, and self-renewing cells including stem cells are the three different types of cells that can be cultivated (Segeritz & Vallier, 2017). Cancer cells can be cultured two-dimensionally (2D) as a monolayer or three-dimensionally (3D). Three D culture has many advantages including a more “physiological” situation and the ability to mimic complex cellular interactions *in vivo* (Kapałczyńska et al., 2018).

Immunofluorescence (IF) staining is a method relying on antibody (Ab)-antigen binding. The target protein can be detected directly by a primary Ab, which is conjugated with a fluorochrome, or indirectly with an unconjugated primary Ab binding the antigen and a secondary, primary Ab-specific Ab coupled to the fluorochrome. The indirect detection method has the advantage that the fluorescence signal can be amplified, but there is also an increased probability of non-specific binding of the secondary Ab.

Immunohistochemistry (IHC) and immunocytochemistry (ICC) are working according to this Ab-antigen principle too. Both approaches are practically the same with the difference that IHC staining is used to visualize target protein in a tissue, whereas ICC is used to detect target protein in individual cells.

Flow cytometry (FC) has its origin in the haemogram analysis where the physical properties of cells are characterized by cell size and cell granularity. Certain cell populations have distinct size and granularity features. The emitted light from a light source is deflected due to cell size and granularity measured with forward and sideward detector, respectively. This basic “cell sorting” approach is extended via the use of fluorescence-labelled Abs to detect specific proteins.

A big advantage of FC over ICC is that autofluorescence can be compensated. Each Ab-coupled fluorochrome has a specific excitation and emission range. In multi-colour experiments the correction of a signal spill-over between different fluorochrome emission spectra is necessary. In addition, some endogenous cell proteins, such as melanin, are known as fluorescent-active agents. Applying the FC compensation features, these overlapped ranges can be corrected by synchronization of signal emission interference of the different fluorochromes to be measured (Adan et al., 2016). By detecting each colourant on its own and measuring the emission of

unstained melanoma cells, the autofluorescence can be subtracted from the emitting signal. ICC does not offer this possibility.

Yet, FC is less applicable for visualisation of the local distribution of a protein on the surface or within a cell and compared to IHC not suitable for assessing 3D cell cultures. Additionally, FC requires much experience in execution and examination. Sensitivity of the methods depends on the application it is used for, but in general FC is able to simultaneously detect several antigens in less time and more cells in one throughput than IHC and ICC.

1.4. Thesis aim

In this thesis, we hypothesize that *in vitro* cultures of cOMM cells harbour a subset of cells displaying a stem cell-like phenotype.

To identify CSCs in cOMM, a total of nine primary cOMM cell lines that have been previously established from patient-derived primary cOMM and cOMM metastases were cultured two-dimensionally, and also grown three-dimensionally into spheres. Then cOMM cells and spheres were analysed by ICC-, IHC- and IF-staining with fluorescent-activated cell sorting (FACS) in double-staining approaches for the presence of CSCs using antibodies specifically binding to CD44 and CD271.

Since CSCs have been previously described as a CD44-positive CD271-positive tumour cell subpopulation within the CD44-positive compartment, we expected to identify cOMM CSCs by this approach.

2. Material and Methods

2.1. Cell culture

A total of nine cOMM cell lines were examined for this thesis (*Table 1*). Until use, they were stored at -150 °C in the Division of Small Animal Internal Medicine. Eight out of nine tumour samples were collected at the Veterinary University of Vienna, the ninth one, Shadow, is a reference sample that was kindly provided by Dr. J.F. Modiano (Koenig et al., 2001).

All the cell lines were thawed quickly at 37 °C and suspended in pre-warmed complete medium (CM) composed of Dulbecco's Modified Eagle's Medium + GlutaMAX™ (DMEM, Life Technologies, Carlsbad, CA, USA), and supplemented with 10 % foetal calf serum (FCS, Life Technologies). The tumour cells were cultivated in a humidified incubator at 37 °C and 5 % CO_2.

Keeping cells in proliferating conditions, they were sub-cultured every third or fourth day. To check on whether these cell lines express CD44 and/or CD271, they were cultured two-dimensionally and three-dimensionally.

Cryopreservation of the cells was conducted to store low passage numbers of each cell line or if a cell line was not needed for the next week. Cells were frozen in Cryomedium composed of DMEM (Life Technologies), 30 % FCS (Life Technologies) and 10 % DMSO (Sigma Aldrich Co., St. Louis, MO, USA), with the determination of cell count was performed on a NucleoCounter®NC-250 (ChemoMetec, Lillerod, Denmark). According to live cell count, cells were resuspended at a density of 2 to 4 × 10^6 cells per 1 ml aliquot in Nunc™ Cryo Tube™ Vials (Thermo Scientific, Waltham, MA, USA). Then, the vials were put in a CoolCell® (BioCision, Mill Valley, CA, USA) to guarantee a gentle cool-down of cells of -1 °C per minute to -80 °C. On the next day vials were transferred to a liquid nitrogen container for long term storage at -150 °C.

All the work procedures with the different cell lines were conducted in a laminar flow cabinet under sterile working conditions to prevent any contamination.

Table 1: Patient and sample properties

Code	Breed	Age	Sex	Tumour type	Diagnosis	Tissue material	Localisation
cRGO1	Mix	11	f	Primary tumour	amelanotic OMM	FNAB	back end hard palate
cRGO1.1				LN metastasis		LN tissue 4cm diameter	right mandibular LN
cRGO1.2				LN metastasis		LN tissue 2cm diameter	left mandibular LN
cRGO2	Mix	15	m	Primary tumour	aggressive, low pigmented OMM	tumour tissue	left caudal mandible
cRGO3	Papillon	11	f	Primary tumour	amelanotic OMM	tumour tissue	right front mandible
cRGO4	Golden Retriever	9	m	Primary tumour	OMM	tumour tissue	right mandible
cRGO5	Cocker Spaniel	11	m	Primary tumour	OMM (III/IVb)	tumour tissue	palate gingiva
cRGO6	Weimaraner	10	f	cutaneous metastasis	amelanotic OMM (III(T2N1M0))	FNAB	multiple skin lesions
Shadow	NA	NA	NA	lung metastasis	OMM; rare cells containing melanin	NA	NA

NA = information not available; FNAB = fine needle aspiration biopsy; LN = lymph node

2.1.1. Two-dimensional Cell Culture

For 2D cultivation (*Figure 1*), the cells were enabled to grow in a T75 culture flask (Thermo Fisher Scientific), using DMEM (Life Technologies), in CM. Subculturing the cells and/or changing the culture medium was done every three to four days at a ratio between 1:3 and 1:15 depending on the proliferation of individual cell lines.

In order to split the cells, the culture medium was removed, and the cell layer was rinsed with Dulbecco's Phosphate Buffer Saline (DPBS, Life Technologies). The addition of Trypsin (0.05 % Trypsin-EDTA (1×), Life Technologies) allowed the detachment of cells. To make sure all the cells were detached, they were monitored under an inverted microscope (Leica DMi1, Leica Microsystems GmbH, Wetzlar, Germany). Once cells were detached completely growth medium was added to the single cells and were resuspended by gentle pipetting. According to the splitting ratio an appropriate aliquot of cell suspension was transferred to a new culture vessel and filled up with complete growth medium to a final volume of 20 ml for T75 flask.

2.1.2. Three-dimensional Cell Culture

The spheroids (*Figure 2*) were cultivated in 96-well U-bottom plates (BRANDplates® inertGrade™ microplates, Brandt Technologies LLC, Bensenville, IL, USA) by seeding 10,000 cells/ well of the cell suspension from the 2D culture. One complete U-bottom plate (Brandt Technologies LLC) was prepared for every single cell line. After splitting the cells like mentioned above, the remaining cell suspension was not discarded but transferred into a 50 ml Falcon™ Tube (Corning, Corning, NY, USA).

In order to seed the right number of cells (cell number per well: 10.000 cells/ 100 µl medium) in the U-bottom plates (Brandt Technologies) they were counted on a NucleoCounter®NC-250 (ChemoMetec). 50 µl cell suspension and 2.5 µl Solution 18 (ChemoMetec), containing acridine orange (AO) and 4',6-diamidino-2-phenylindole (DAPI) for the detection of viable and dead cells were mixed and 10 µl of the mixture was put in the counting chamber. According to the obtained cell count a cell suspension was created containing 1.100.000 cells/ 11 ml by diluting with the required volume of CM. In each well of a 96-well U-bottom plate 100 µl of this suspension was pipetted for each cell line. The plates were incubating at 37 °C and 5 % CO_2 for 7 days. After 5 days 100 µl of CM was added to every well.

2.2. Immunocytological staining

Melanoma cell lines were split as described in 2.1.1 and seeded in 8-well chamber slides (Ibidi, Gräfelfing, Germany) for immunocytological staining in 2D culture. Before seeding the chamber slides had to be coated for better cell adhesion with Poly-D-Lysin (Thermo Fisher Scientific). The seeded cell suspension had a concentration of 90.000 cells/ ml. Cell count was performed as described above. The chamber slides were incubated at 37 °C and 5 % CO_2 for 24 hours. After incubation the medium was removed, the cells were washed with DPBS (Life Technologies) and fixated with 4 % buffered formaldehyde (SAV Liquid Production GmbH, Flintsbach am Inn, Germany) followed by further washing steps, once with DPBS (Life Technologies) and twice with distilled filtered water. The air-dried chamber slides were ready for staining.

A first staining approach with the cell lines cRGO1, cRGO4 and Shadow was done as two of them were positive for CD271 in earlier experiments. Per cell line two 8-well chamber slides were made, to have sufficient wells for titration of antibodies for single and double staining.

Air-dried chamber slides were rehydrated with 1 × PBS (for 10 ×: 90 g NaCl, 11.4 g Na_2HPO_4, 2.8 g NaH_2PO_4, filled up to 1 L with H_2O and diluted to 1 × solution). PBS was added to each well and incubated for seven minutes. This step was repeated twice. Then, 50 µl of 1.5 % goat serum (Sigma Aldrich Co.) in PBS was applied to each well to block any unspecific antibody-protein binding reactions of the primary Abs. This is done by occupying the non-specific proteins that may bind the used primary Abs with the blocking serum's own Abs. After an incubation for 30 minutes the primary Abs were added (*Table 2*).

Different concentrations of primary Abs were applied in the chambers to evaluate the necessary concentration. CD44 Abs were diluted 1:250, 1:500 and 1:1000, and CD271 1:200, 1:400 and 1:800. The same concentrations were used for the double staining assay. Chamber slides with the primary Abs were incubated at room temperature overnight. On the following day the chambers were washed three times with PBS (1 ×) for five minutes. According to primary Ab the corresponding secondary Ab was added (*Table 2*). Afterwards cells were washed with PBS (1 ×) twice for five minutes before staining the nuclei with DAPI (Sigma Aldrich Co.) for five minutes and then washing twice with distilled water. The chambers could now be removed from

the slide and a coverslip was mounted with Aqua-Poly/Mount (Polysciences Inc., Warrington, PA, USA) to protect the cells.

This approach was not effective enough as the used Abs did not provide evaluable results because of a very strong autofluorescence signal of the cell lines. After redoing the experiment with cRGO6 and A-375 (ATCC, Manassas, VA, USA), a human melanoma cell line, we obtained similar results, even after changing the secondary Ab to one with a more distant emission spectrum. For this reason, we decided changing to FACS for the assessment of the 2D cultured cells, where autofluorescence can be compensated.

2.3. Flow cytometry

For FACS analysis the different melanoma cell lines were counted like mentioned in 2.1.2. Counted cells were collected in a 50 ml Falcon™ tube (Corning), washed twice and then resuspended in 10 ml DPBS (Life Technologies). Cells were split as mentioned above, with the only difference that instead of Trypsin (Life Technologies) Accutase (Stemcell Technologies, Vancouver, BC, Canada) was used, because it is less damaging and more gentle to the cells leading to an increased viability.

For live/death (L/D) staining suspensions containing ~ 500 000 cells were transferred in a 1.5 ml tube and then incubated at 65 °C for 2 min to destroy the cells. After cooling down the same number of live cells (~ 500 000 cells) were added to the dead.

Shortly after, Fc-Block (1:100, Fc Receptor Binding Inhibitor for dog, Invitrogen, Waltham, MA, USA)-, anti-CD44 Ab (1:100)-, anti-CD271 Ab (1:100)-, L/D staining solution (1:100, APC-Cy7 LIVE/DEATH™, Invitrogen) and a master mix (1:100) containing anti-CD44, anti-CD271 Abs and L/D staining solution were prepared. Used Abs can be taken from *Table 2* and DPBS (Life Technologies) was used for dilution.

The investigated cell lines were put into the wells of a V-bottom microtiter plate (Greiner Bio-One 96-well plate, Kremsmünster, Austria) to facilitate the workflow. Appropriate number of wells were prepared by applying 1×10^6 cells per well. Then Fc-Block (Invitrogen) was applied to each well and incubated for 15 min at 4 °C, except for the unstained control cells where only DPBS (Life Technologies) was added.

Later, the prepared staining solutions were applied and incubated for 60 min at 4 °C in the wells. At the same time compensation beads were prepared by mixing 200 µl DPBS (Life Technologies) with one droplet of the compensation bead solution (UltraComp eBeads™ Compensation Beads, Invitrogen) and the prepared antibody-staining solutions (1:200), one vial with anti-CD44, one with anti-CD271 and one with L/D staining and then incubated for 30 min in the dark. The beads, as well as the Ab-stained cells were washed several times, spined down and then resuspended in DPBS, containing 3 % FCS (both Life Technologies). All the samples were then transferred in a FACS tube (Sarstedt, Nümbrecht, Germany) by filtering them through a 100 µm Falcon™ cell strainer (Corning) and acquired on a BD FACSCanto™ II (BD Biosciences, Franklin Lakes, NJ, USA).

2.4. Immunohistological staining

All the cultured spheroids from every well of a U-bottom plate (Brandt Technologies) were transferred in a 15 ml Falcon™ (Corning) tube each. The supernatant was aspirated, and the spheroids were washed with DPBS (Life Technologies) and fixated in 4 % buffered formaldehyde (SAV Liquid Production GmbH).

Paraffinizing the spheroids was done with the VetCore Facility (VetImaging/ VetBiobank) of the University of Veterinary Medicine Vienna. For this, the cells were processed with the HistoGel™-kit (Thermo Scientific) before putting the spheroids in an ascending alcohol series, ending with xylene (ACM-Herba Chemosan Apotheker AG, Vienna, Austria), and then in paraffin (Sanova Pharma, Vienna, Austria) using for this entire process a vacuum infiltration processor (Tissue-Tek®VIP® 6, Sakura Finetek, Alphen aan den Rijn, NL).

Formalin-fixed-Paraffin-embedded blocks were cut in 3-5 µm sections and then rehydrated for staining, using a decreasing alcohol series, starting with xylene (ACM), followed by lowering ethanol (LS Dienstleistungen GmbH, Gerasdorf, Austria) concentrations and ending with distilled water. Then, for heat induced epitope retrieving, slides were treated at pH 6 with citrate buffer (0.01 M; for 0.1 M: 2.1 g $C_6H_8O_7 \times H_2O$, 800 ml distilled water, setting pH with 2 M NaOH, fill up to 1 L with water) in a steamer for 30 min. After cooling down, slides were washed with PBS (1 ×) twice, then blocking was done with 1.5 % goat serum (Sigma Aldrich Co.) in PBS and incubated for 30 min before applying the primary Abs (*Table 2*), which stayed on the histological cuts overnight.

On the next day, primary Abs were removed, secondary Abs (*Table 2*) added and incubated for one hour, nuclei stained with DAPI (Sigma Aldrich Co.) and in between those steps washed with PBS (1 ×). After staining with DAPI slides were washed with distilled water and a cover slip was mounted with Aqua-Poly/Mount (Polysciences Inc.). Dried slides could be investigated under a microscope.

Different combinations and concentrations of Abs were used to minimize autofluorescence but still get appropriate results. Therefore, Abs, both anti-CD271 and anti-CD44 were assessed in 1:250, 1:500 and 1:1000 dilutions and a no primary (Ab) control (NPC) with different secondary Abs (*Table 2*).

Additionally, haematoxylin/eosin (H/E) stained histological slides were prepared for better visualisation of the spheroids. At first, spheres were rehydrated in a decreasing alcohol series, then stained with haematoxylin (Epredia, Kalamazoo, MI, USA) and washed with water, before staining with eosin (Merck, Darmstadt, Germany) and dehydrating them with an ascending alcohol series. Coverslips were mounted with Consul-Mount^{TM} (Epredia) on the slides (Epredia).

Table 2: Antibody specifications

	Antibody host	Antibodies	Manufacturer (catalogue nr.)
Immunocytological staining			
Primary Abs	Rat	Anti-CD44 (IM7)	Santa Cruz Biotechnology (sc-18849); Dallas, TX, USA
	Rabbit	Anti-CD271 (D4B3)	Cell Signaling (8238); Danvers, MA, USA
Secondary Abs	Goat	Anti-rat (A488)	Invitrogen (A11006); Waltham, MA, USA
	Goat	Anti-rabbit (A546)	Life Technologies (A11035)
	Donkey	Anti-rabbit (A680)	Jackson Immuno Research (711-625-152); Bar Harbor, ME, USA
Immunohistological staining			
Primary Abs	Rat	Anti-CD44 (IM7)	Santa Cruz Biotechnology (sc-18849)
	Rabbit	Anti-CD271 (D4B3)	Cell Signaling (8238)
Secondary Abs	Goat	Anti-rat (A488)	Invitrogen (A11006)
	Goat	Anti-rat (A+488)	Invitrogen (A48262TR)
	Donkey	Anti-rabbit (A488)	Invitrogen (A11034)
	Goat	Anti-rabbit (A568)	Invitrogen (A11011)
	Goat	Anti-rabbit (A680)	Jackson Immuno Research (711-625-152)
Flow cytometry			
PerCP Cy5.5 labelled primary Ab	Rat	Anti-CD44 (IM7)	Thermo Fischer Scientific (45-0441-82)
APC labelled primary Ab	Mouse	Anti-CD271 (ME20.4-1.H4)	Miltenyi Biotec (130-113-418); Bergisch Gladbach, Germany

3. Results

3.1. Cell culture

3.1.1. Two-dimensional Cell Culture

To show that most of the cell lines exhibit different morphology in 2D, light microscopic images (*Figure 1*) were taken with Leica DMi8 (Leica Microsystems GmbH). For example, cRGO5 is showing giant inflated cells, while cRGO1.2 and cRGO2 are able to form spheroids in 2D.

To make these pictures, the cells had to be seeded as mentioned in 2.1.2. in a 6-well plate (Biologix Group Limited, Hallbergmoos, Germany) at a cell number of 500.000 cells/ well.

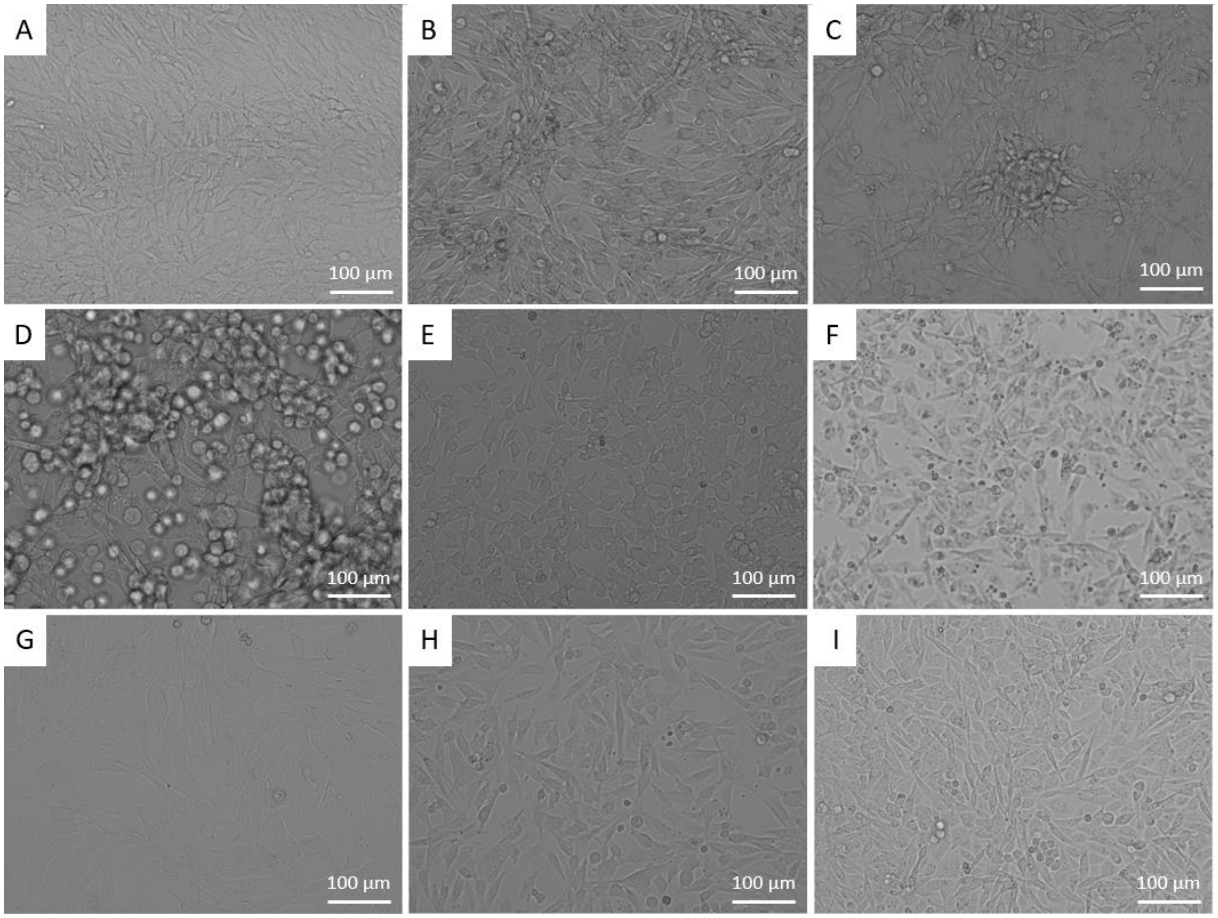

Figure 1: Light microscopic images of the different cell lines in 2D cultivation. Pictures A to I are corresponding to the order of *Table 1* (cRGO1, cRGO1.1, cRGO1.2, cRGO2, cRGO3, cRGO4, cRGO5, cRGO6, Shadow). Cells in picture *C* and *D* showing self-assembly of spheroids in 2D culture.

3.1.2. Three-dimensional Cell Culture

To verify that all the cell lines were indeed able to form spheroids in U-bottom plates (Brandt Technologies LLC), light microscopic images (*Figure 2*) were taken with Leica DMi8 (Leica Microsystems GmbH).

Like in 2D cultivation cell lines have different appearances compared to each other. Cells in cRGO2 and Shadow do not attach as dense, while spheroids in cRGO1 and cRGO5 are much smaller and denser. Spheroids in cRGO4 and cRGO6 have protuberances.

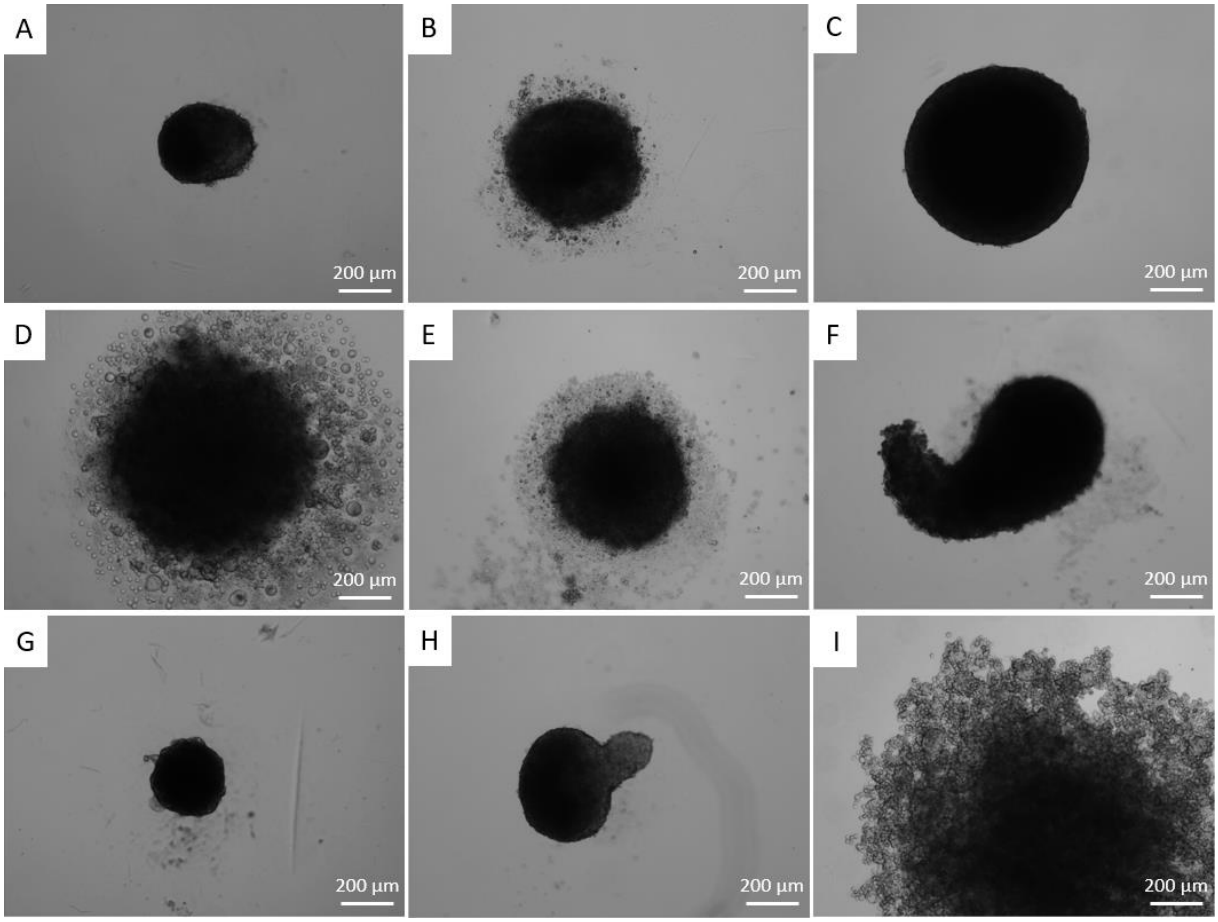

Figure 2: Light microscopic images of the different cultivated spheroids seven days after seeding. Pictures A to I are corresponding to the order of *Table 1* (cRGO1, cRGO1.1, cRGO1.2, cRGO2, cRGO3, cRGO4, cRGO5, cRGO6, Shadow). Depicted spheroids from every cell line are representative for all the other in U-bottom plates seeded cells and most of the different cell lines had unique appearances.

3.2. Flow cytometry

Flow cytometry was carried out with BD FACSCanto™ II (BD Biosciences) and the BD FACSDiva™ Software v9.0 (BD Biosciences) and FloJo™ v10 (BD Biosciences) was used for analysis of the results. Final concentrations of the labelled Abs were 1:200.

At first, the sought-after population had to be gated within the forward- side scatter diagram, which excluded the cellular debris and the duplicates. Then, only the viable cells were taken for evaluation of CD44 and CD271.

As depicted in *Figure 3* nearly all the cells in every cell line are CD44-positive. Additionally, only samples cRGO1, cRGO3 and A-375 are positive for CD271, with cRGO3 and A-375 having very high percentages of CD44+/CD271+ cells (*Table 3*). Gating for all the single stained cell lines was done manually, thus all the values ~ 1 % or below should not be embraced.

Table 3: Percentages of cell populations

Cell line	**CD44**+/CD271-	CD44-/**CD271**+	**CD44+/CD271+**	CD44-/CD271-
cRGO1	78,7 %	1,36 %	12,6 %	7,40 %
cRGO1.1	99,2 %	0 %	3,60E-3 %	0,8 %
cRGO1.2	97,0 %	0 %	0,049 %	2,92 %
cRGO2	87,4 %	3,61E-3 %	3,61E-3 %	12,6 %
cRGO3	2,40 %	5,91 %	86,7 %	4,96 %
cRGO4	78,1 %	0,029 %	0,14 %	21,8 %
cRGO5	98,1 %	1,77E-3 %	0,31 %	1,57 %
cRGO6	93,1 %	8,50E-3 %	0,086 %	6,79 %
Shadow	96,7 %	0 %	1,38E-3 %	3,3 %
A-375	18,4 %	0,46 %	78,3 %	2,83 %

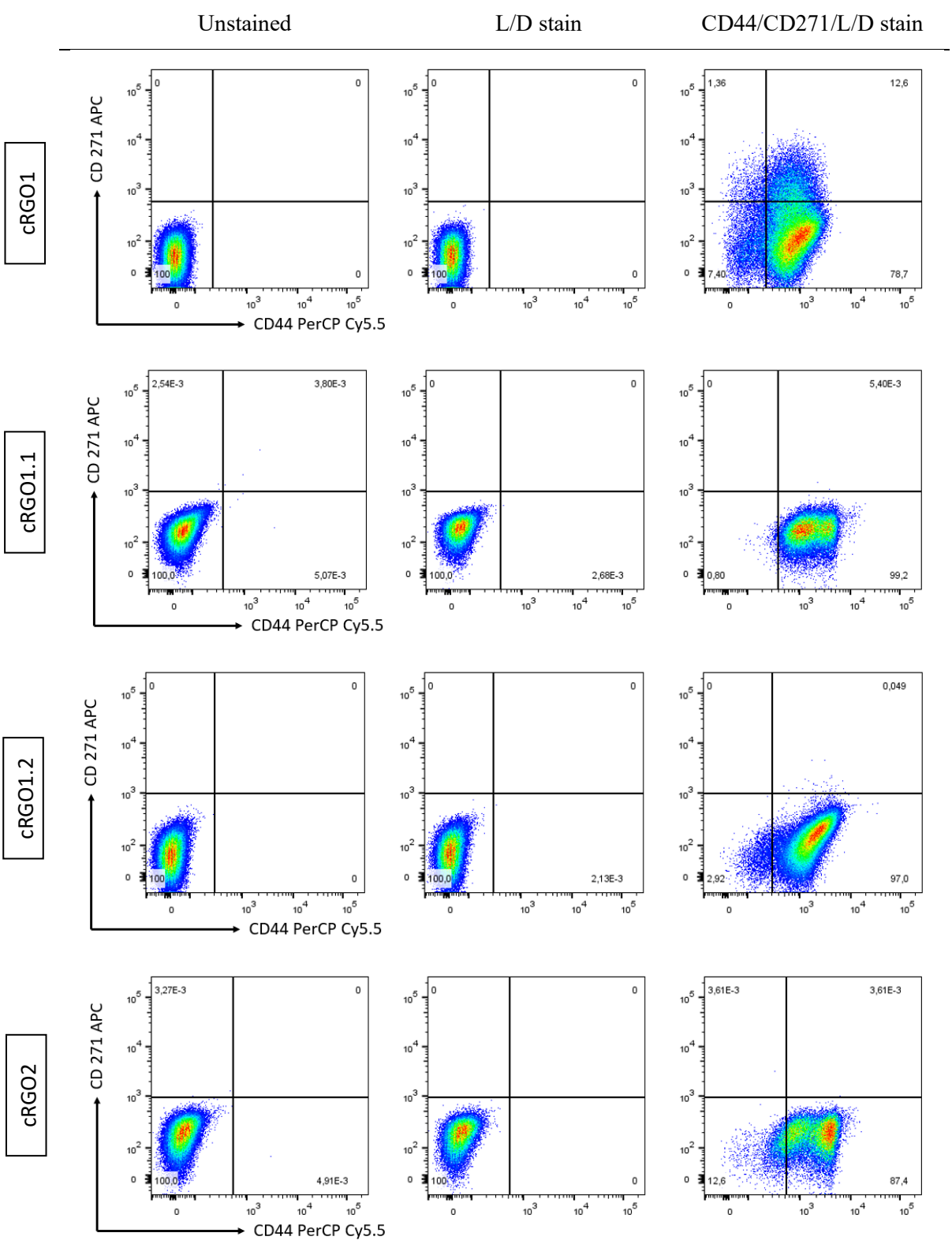
Unstained
L/D stain
CD44/CD271/L/D stain
cRGO1
cRGO1.1
cRGO1.2
cRGO2
CD 271 APC
CD44 PerCP Cy5.5
0
100
1,36
12,6
7,40
78,7
2,54E-3
3,80E-3
100,0
5,07E-3
2,68E-3
5,40E-3
0,80
99,2
0,049
2,92
97,0
2,13E-3
3,27E-3
4,91E-3
3,61E-3
12,6
87,4

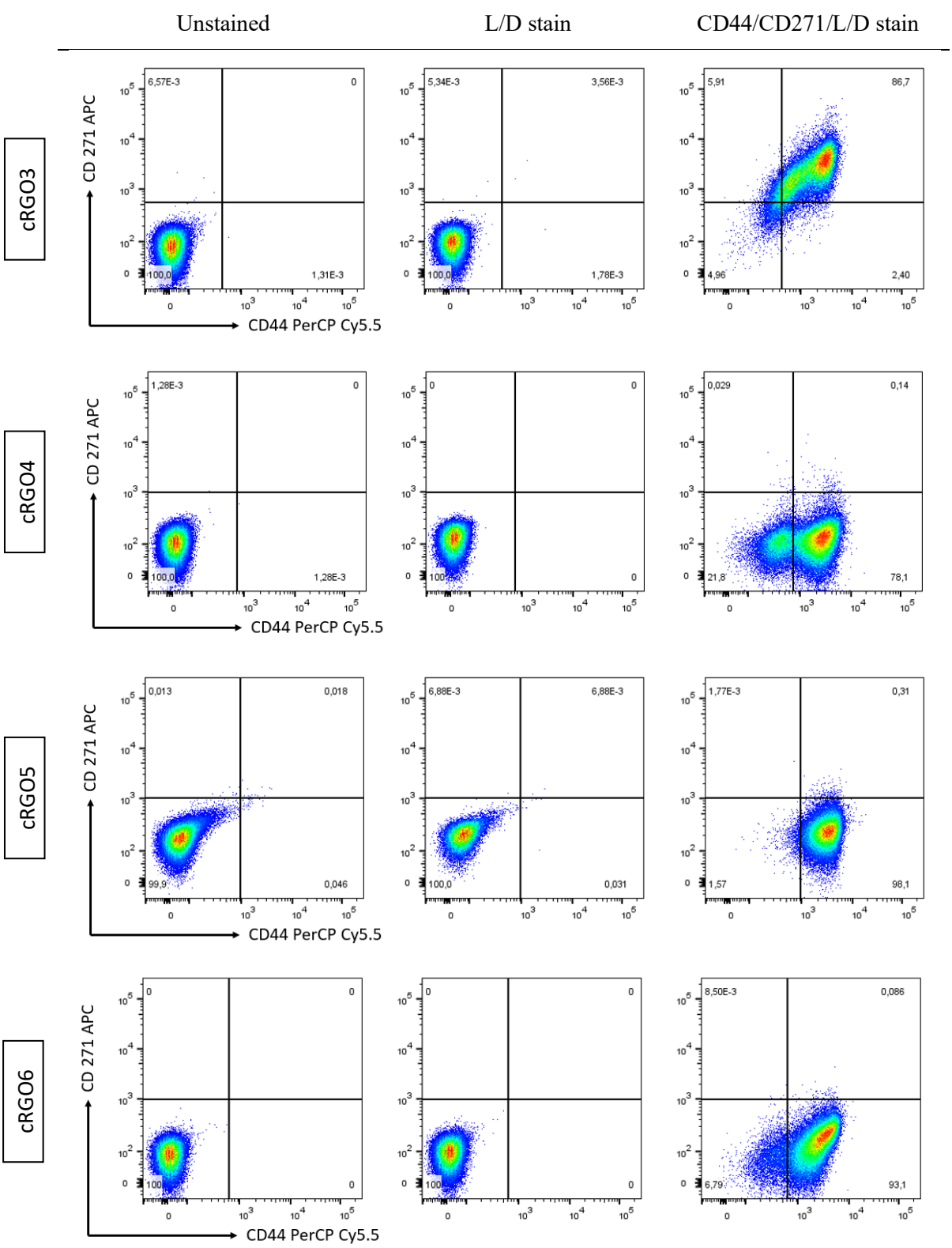
Unstained
L/D stain
CD44/CD271/L/D stain
cRGO3
cRGO4
cRGO5
cRGO6
CD 271 APC
CD44 PerCP Cy5.5
6,57E-3
0
100,0
1,31E-3
5,34E-3
3,56E-3
100,0
1,78E-3
5,91
86,7
4,96
2,40
1,28E-3
0
100,0
1,28E-3
0
0
100
0
0,029
0,14
21,8
78,1
0,013
0,018
99,9
0,046
6,88E-3
6,88E-3
100,0
0,031
1,77E-3
0,31
1,57
98,1
0
0
100
0
0
0
100
0
8,50E-3
0,086
6,79
93,1

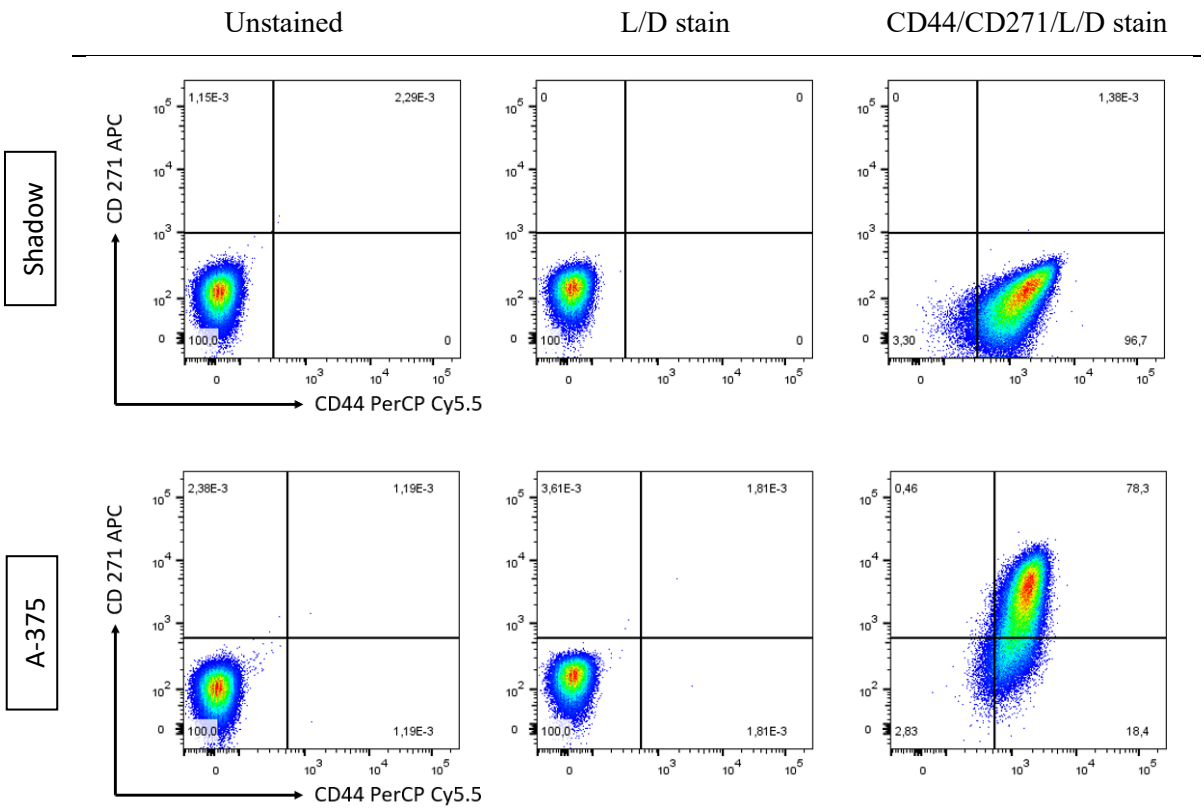

Figure 3: Flow cytometry results of the nine cOMM samples and the human malignant melanoma sample A-375 as a reference. Left pictures showing unstained-, middle pictures only L/D-stained- and right pictures CD44- and CD271 Abs and live/death-stained samples. Unstained- and L/D-stained diagrams are depicted to demonstrate that after gating all cells from every cell line were alive when assessed for CD44 and/or CD271 expression. Lower left quadrant (q) in every diagram shows CD44−/CD271−, lower right q CD44+/CD271−, upper left q CD44−/CD271+ and upper right q CD44+/CD271+ cells and is dependent on the intensity of the signal that is absorbed, emitted by the fluorochromes APC (y-axis) and PerCP Cy5.5 (x-axis).

3.3. Immunohistological staining

Histological slides were investigated with Zeiss Axio Imager Z2 (Carl Zeiss AG, Oberkochen, Germany) and ZEN v3.4 (Carl Zeiss AG) software. Final concentrations of the primary Abs in double-staining were 1:500 (anti-CD44; rat) and 1:150 (anti-CD271; rabbit), in single staining 1:500 (anti-CD44; rat) and 1:240 (anti-CD271; rabbit), and of the secondary Abs 1:500 (A+488; anti-rat) and 1:250 (A680; anti-rabbit).

After the failed ICC approach due to the strong autofluorescence signal, we investigated at first at which exposure time some cell lines emit a wrong positive signal. For that, we also checked if a primary Ab exhibited a wrong signal in a secondary Ab mix (both anti-rat Ab and anti-rabbit Ab) for the non-corresponding secondary Ab.

Because melanin has a similar emission spectrum like our CD44-signal, a very weak CD44-positive signal could be detected at an exposure time of over 1 s. for CD271-single-stained samples. But as the expression of CD44 in the cells is high, we only evaluated fluorescence-signals at an exposure time under 100 ms.

The expression of CD271, if it was present, was extremely low. Most of the cell lines showed a poor CD271-colouring for CD44-single-staining at an exposure time over 2 s., which looked identically to the CD44-signal. Therefore, we only declared samples CD271-positive, which featured not-CD44-identical signals at an exposure time under 1 s.

All the cell lines were CD44-positive, but only two of them were positive for CD271. CD271-positive samples in flow cytometry cRGO3 and A-375, which are CD271-negative in IHC-staining are shown in *Figure 4*, cRGO1 which is CD271-postive in both approaches in *Figure 5*, and cRGO1.1, which is CD271-positive in IHC in *Figure 6*. CD44 expression is highest on the cell surface and CD271 expression in both, cell surface-and cytoplasm.

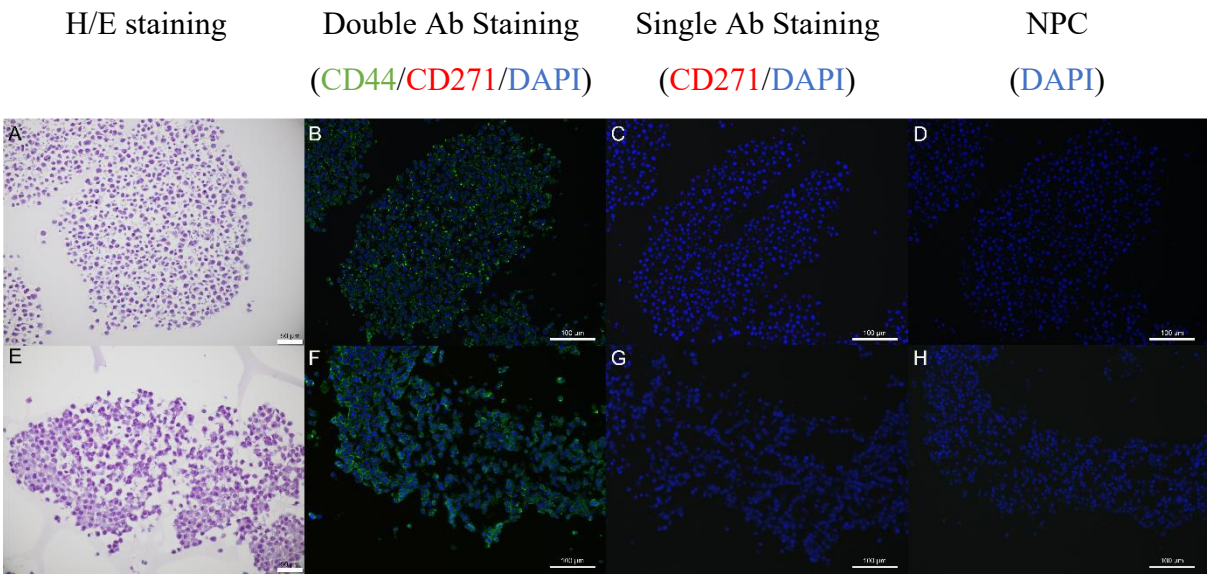

Figure 4: Representative light microscopic and epifluorescence pictures (*B-D* and *F-H,* scale bar 100 µm) for all the CD271-negative spheroids. cRGO3 results are shown in *A-D* and A-375 in *E-H.* Spheroids in pictures *A* and *E* (scale bar 50 µm) were H/E stained (nuclei violet-blue, cytoplasm pink). A-375 shows a more ruptured morphology than all the other cell lines. *B* and *F* are depicting double-staining for both markers, whereas *C* and *G* only single-staining for CD271. Single staining for CD44 is not shown because it would be identically to *B* and *F*. NPCs can be seen in *D* and *H*, looking alike *C* and *G*. Nuclei were visualized with DAPI (blue). CD44-Alexa 488 produces a green signal.

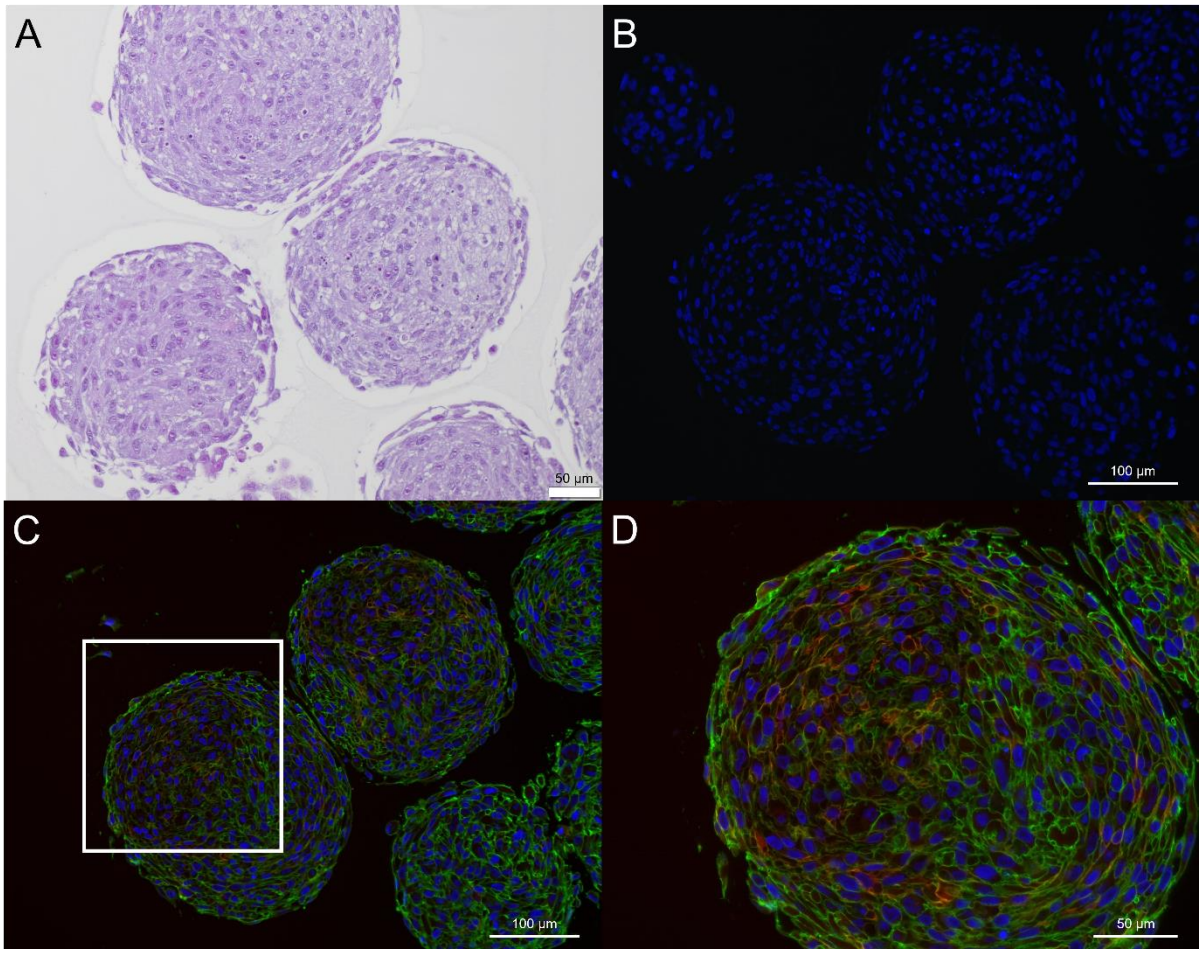

Figure 5: Light microscopic (*A*) and epifluorescence pictures (*B-D*) of the cRGO1 spheroids. H/E-staining in *A* (scale bar 50 µm) shows that the outer cells of the spheroids are tightly clutched and flattened holding the spheroid together. Little dark spots in the centre are tightly packed heterochromatin indicating necrosis. Picture *C* (scale bar 100 µm) and *D* (scale bar 50 µm) are showing double staining for both markers, but *D* with a higher magnification. Single staining for CD44 and CD271 are not shown as they look like the double staining. *B* (scale bar 100 µm) shows NPC. Nuclei were visualized with DAPI (blue). CD44-Alexa 488 produces a green signal, and CD271-Alexa 680 is shown with a red signal.

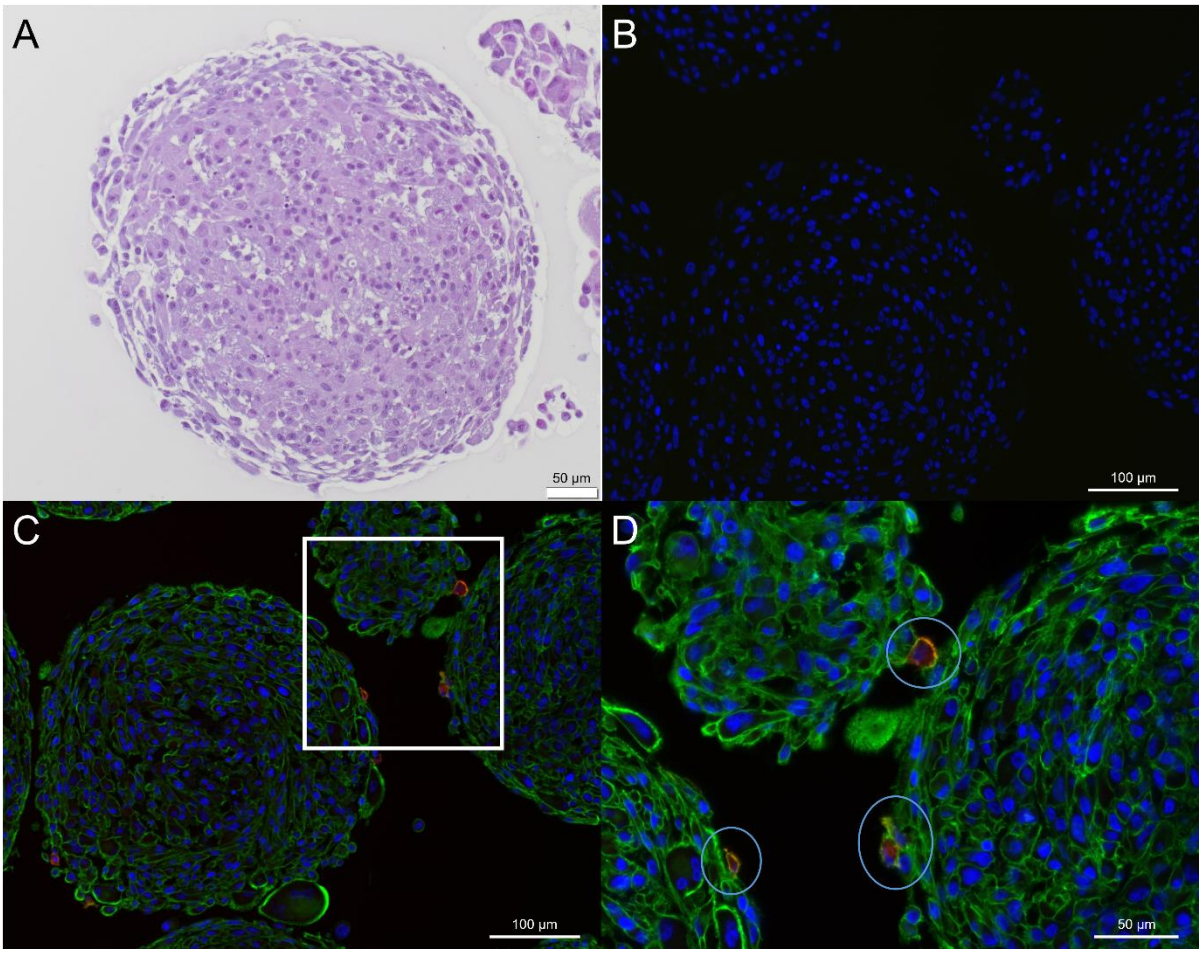

Figure 6: Light microscopic (*A*) and epifluorescence pictures (*B-D*) of the cRGO1.1 spheroids. *C* (scale bar 100 µm) and *D* (scale bar 50 µm) are showing double staining for both markers, but with a different magnification, *B* (scale bar 100 µm) for NPC. Single staining for CD44 and CD271 are not shown. CD44 expression is generally very high on the cell surface, while CD271 expression is cytoplasmic and compared to cRGO1 also very high on the surface, so that the signal can even be seen despite the strong signal from CD44. Nuclei were visualized with DAPI (blue). CD44-Alexa 488 produces a green signal, and CD271-Alexa 680 is shown with a red signal.

4. Discussion

CSCs are a promising target to study the complexity of tumour biology *in vitro*. By investigating different CSC markers, more information will be available to finally win the fight against cancer.

One must keep in mind that while different markers can be found in *in vitro* cultures in excess, *in vivo* the tumour cells exhibit only low percentages of the same populations, and their tumorigenic potential is, for example due to plasticity, highly dependent on the cells' microenvironment (Boumahdi & de Sauvage, 2019; Meacham & Morrison, 2013). 2D and 3D culture show us that within the same diagnosed cancer, differences in morphology can occur. Even within the same individual, primary and metastatic tumours might have different properties, for example cRGO1.2 showed resistance to irradiation in earlier experiments compared to cRGO1 and cRGO1.1, which were highly radiosensitive.

Our results show that CSC markers CD44 and CD271 can be found in 2D cultivated cOMM cells. Whereas CD44 was highly expressed by all the cell lines, CD271 expression only occurred in three of them, with most of the CD271-positive cells residing within the CD44-positive cell compartment, as already described (Elkashty et al., 2020). The three CD271-positive cell lines were all derived from primary tumour tissue. Interestingly, primary cRGO1 harboured CD271-positive cells, while lymph node metastases cRGO1.1 and cRGO1.2 did not, indicating that cell properties changed in the course of metastasis.

CD271 is a marker also associated with brain metastases. Thus, it might be possible that the location where a primary tumour can metastasise to is predetermined by its expression profile. For example, A-375, a quite well investigated human malignant melanoma cell line, exhibited a high percentage of CD271-positive cells, and was observed in *ex-vivo* brain samples (Radke et al., 2017).

Most interestingly in our study were the cell lines cRGO1, cRGO1.1 and cRGO1.2, which were all extracted from the same dog. Primary cOMM cell line cRGO1 exhibited CD271-positive cells in 2D and 3D. Metastases cRGO1.1 expressed CD271 only in 3D, and cRGO1.2 expressed no CD271 at all. This led to the theory that metastasis to lymph nodes does not necessitate CD271. However, when stimulated to form spheres, as is the case during EMT, cRGO1.1

started expressing CD271 again (Chen et al., 2017). This event and the bigger size of the lymph node metastasis from which cRGO1.1 cells were explanted (*Table 1*) indicate that this metastasis had undergone MET to firmly establish itself in the lymph node (Schmid et al., 2019). In comparison, this may not apply to the smaller metastasis from which cRGO1.2 originated. This metastasis may not have fully settled at the point in time of biopsy.

On the other hand, A-375 and cRGO3 were shown to be CD271-positive in 2D but not in spheroids. Saltari and her colleagues stated that down-regulation of CD271 promotes melanoma progression and invasion. They demonstrated that primary melanoma expresses more CD271 than metastatic melanoma and an increased ability of CD271-negative cells to metastasize compared to CD271-positive cells in zebrafish (Saltari et al., 2016). Another explanation would be less biological than technical. By fixation of the histological slides, preservation of epitopes and their immunoreactivity can be achieved, but at the same time other epitopes might be degraded or masked (Im et al., 2019). That might even be more likely as CD271 expression is reported to be cytoplasmic (Strohmayer et al., 2022).

The only primary cell line harbouring a CD44-negative CD271-positive cell subpopulation was cRGO3. Whether this CD44-negative cell fraction also corresponds to CSCs remains unclear. CD44-positive tumour cell populations show more resistance to oxidative stress, and after xenograft implantation, mice exhibited worse clinical outcome when the CD44-positive population was increased (Diehn et al., 2009; Joshua et al., 2012). CD44 expression has generally become highly associated with various kinds of cancers, for example in breast, bladder, head and neck squamous cell carcinoma and melanoma. However, that might be because CD44 occurs in normal stem cells and cancer cells as well (Morath et al., 2016; Yan et al., 2015).

Tumour heterogeneity and cell plasticity make it difficult to investigate cancers and CSCs, but eventually there must be a pattern or hierarchy between tumorigenic and non-tumorigenic cells. Targeting these cells with tumorigenic potential might lead to health recovery (Frank et al., 2010; Meacham & Morrison, 2013). For example, it was shown that Ab therapy in combination with targeting CD271-positive cells could inhibit melanoma metastasis (Ngo et al., 2016).

In conclusion, it is necessary to gather as much information as possible on the presence of diverse CSC markers for various cancers in different hosts. In this thesis, we examined two promising CSC markers and showed that CD44-positive CD271-positive cells can be found in cOMM. In depth-studies will help confirm their identity and clarify their role in this dreaded canine disease.

5. Summary

Epithelial-mesenchymal transition (EMT) is a process, where epithelial cells lose their typical properties but gain mesenchymal characteristics. Additionally, EMT is associated with a process that promotes the transition of epithelial tumour cells to a cancer stem cell (CSC) like phenotype. CSCs share typical stem cell properties such as self-renewal and multidirectional differentiation. Furthermore, they are resistant to stress factors such as DNA damage or chemo- and radiation therapy.

Canine oral malignant melanoma (cOMM) has a high metastatic potential and is a common malignancy in dogs. In cOMM, only scarce information is available on the presence and pathogenic role of CSCs. Therefore, we assessed cOMM cells for expression of two different clusters of differentiation, i.e., CD44 and CD271, that are confirmed markers for human CSCs. CD44 is a very abundant marker for CSCs in general, and CD271 is one that relates to metastases, especially in the brain. It is currently assumed that CSCs are CD271-positive cells within the CD44-positive cell compartment, which are hyperproliferating and show higher resistance to treatment than CD44-positive CD271-negative cells.

To identify CSCs in cOMM, a total of nine primary cOMM cell lines that have been previously established from patient-derived primary cOMM and cOMM metastases were cultured in 2D and 3D (spheres). COMM cells and spheres were analysed by immunocyto- and immunohistochemical staining and flow cytometry using antibodies specifically binding to CD44 and CD271.

CD44-positive cells were detected in all nine cOMM cell lines. CD271 was expressed in three 2D- and two 3D cultured cell lines, of which only one, cRGO1, contained a CD44-positive CD271-positive subpopulation in both cultivation systems. This suggests that during EMT potential CSC properties can change depending on which influences the cells are exposed to.

6. Zusammenfassung

Epithelial-mesenchymale Transition (EMT) ist ein Prozess, in dem Epithelzellen ihre typischen Eigenschaften verlieren und jene von Mesenchymzellen erlangen. Des Weiteren ist mit diesem Prozess auch ein sekundärer Prozess miteingeschlossen, welcher die Transition von Epithelzellen zu einem Tumor-Stammzellen ähnlichen Phänotyp beinhaltet. Diese sind, wie normale Stammzellen, in der Lage sich in verschiedenste Zelltypen zu differenzieren, sich selbst zu erneuern und besitzen die Fähigkeit gegen verschiedenste Stressfaktoren resistent zu sein.

Das bösartige orale Melanom in Hunden neigt dazu sich gerne zu verstreuen und kommt häufig vor. Da nur wenig über das Vorhandensein und der Pathogenität von Tumor-Stammzellen bei oralem Melanom in Hunden bekannt ist, untersuchten wir zwei Oberflächenmerkmale, die bereits im Zusammenhang mit Tumor-Stammzellen stehen. CD44 ist ein allgemein häufig in Tumor-Stammzellen vorkommendes Protein und CD271 eines, welches mit Metastasen, insbesondere welchen im Gehirn in Verbindung steht. Zusätzlich wurde argumentiert, dass CD271-positive Zellen eine Subpopulation innerhalb der CD44-positiven Zellen sind, welche ausgeprägtere Resistenzen gegen Therapien aufweisen und schneller wachsen können.

Um orales Melanom von Hunden auf die beiden Oberflächenmerkmale zu testen, wurden neun Zelllinien, darunter Primärtumorzellen und Zellen aus Metastasen, zwei- und dreidimensional kultiviert. Anschließend konnten sie mit Immunfärbungen mit FACS und histologischen Methoden analysiert werden.

Ergebnisse zeigten, dass alle getesteten Zelllinien positiv auf CD44 waren. CD271-positive Zellen konnten dreimal in 2D Kultur und zweimal in 3D Kultur detektiert werden. Nur eine der neun Proben, cRGO1, wies sowohl in 2D-, als auch in 3D Kultur auf eine CD44- und CD271-positive Subpopulation hin. Dies lässt rückschließen, dass sich während EMT die Tumorstammzell-Eigenschaften abhängig von verschiedenen Einflüssen ändern können.

7. References

Adan, A., Alizada, G., Kiraz, Y., Baran, Y., & Nalbant, A. (2016). Flow cytometry: basic principles and applications. *Https://Doi.Org/10.3109/07388551.2015.1128876*, *37*(2), 163–176. https://doi.org/10.3109/07388551.2015.1128876

Almela, R. M., & Ansón, A. (2019). A Review of Immunotherapeutic Strategies in Canine Malignant Melanoma. *Veterinary Sciences 2019, Vol. 6, Page 15*, *6*(1), 15. https://doi.org/10.3390/VETSCI6010015

Atherton, M. J., Morris, J. S., McDermott, M. R., & Lichty, B. D. (2016). Cancer immunology and canine malignant melanoma: A comparative review. *Veterinary Immunology and Immunopathology*, *169*, 15–26. https://doi.org/10.1016/J.VETIMM.2015.11.003

Bergman, P. J. (2007). Canine Oral Melanoma. *Clinical Techniques in Small Animal Practice*, *22*(2), 55–60. https://doi.org/10.1053/J.CTSAP.2007.03.004

Boiko, A. D., Razorenova, O. v., van de Rijn, M., Swetter, S. M., Johnson, D. L., Ly, D. P., Butler, P. D., Yang, G. P., Joshua, B., Kaplan, M. J., Longaker, M. T., & Weissman, I. L. (2010). Human melanoma-initiating cells express neural crest nerve growth factor receptor CD271. *Nature 2010 466:7302*, *466*(7302), 133–137. https://doi.org/10.1038/nature09161

Boumahdi, S., & de Sauvage, F. J. (2019). The great escape: tumour cell plasticity in resistance to targeted therapy. *Nature Reviews Drug Discovery 2019 19:1*, *19*(1), 39–56. https://doi.org/10.1038/s41573-019-0044-1

Cervantes-Arias, A., Pang, L. Y., & Argyle, D. J. (2013). Epithelial-mesenchymal transition as a fundamental mechanism underlying the cancer phenotype. *Veterinary and Comparative Oncology*, *11*(3), 169–184. https://doi.org/10.1111/J.1476-5829.2011.00313.X

Chan, M. M., & Tahan, S. R. (2010). Low-affinity nerve growth factor receptor (P75 NGFR) as a marker of perineural invasion in malignant melanomas. *Journal of Cutaneous Pathology*, *37*(3), 336–343. https://doi.org/10.1111/J.1600-0560.2009.01349.X

Chen, T., You, Y., Jiang, H., & Wang, Z. Z. (2017). Epithelial–mesenchymal transition (EMT): A biological process in the development, stem cell differentiation, and tumorigenesis. *Journal of Cellular Physiology*, *232*(12), 3261–3272. https://doi.org/10.1002/JCP.25797

Chinn, S. B., Darr, O. A., Owen, J. H., Bellile, E., McHugh, J. B., Spector, M. E., Papagerakis, S. M., Chepeha, D. B., Bradford, C. R., Carey, T. E., & Prince, M. E. P. (2015). Cancer stem cells mediate tumorigenesis and metastasis in head and neck squamous cell carcinoma. *Head & Neck*, *37*(3), 317. https://doi.org/10.1002/HED.23600

Civenni, G., Walter, A., Kobert, N., Mihic-Probst, D., Zipser, M., Belloni, B., Seifert, B., Moch, H., Dummer, R., van den Broek, M., & Sommer, L. (2011). Human CD271-positive melanoma stem cells associated with metastasis establish tumor heterogeneity and long-term growth. *Cancer Research*, *71*(8), 3098–3109. https://doi.org/10.1158/0008-5472.CAN-10-3997/649807/AM/HUMAN-CD271-POSITIVE-MELANOMA-STEM-CELLS

Davies, A. M., Bandtlow, C., Heumann, R., Korsching, S., Rohrer, H., & Thoenen, H. (1987). Timing and site of nerve growth factor synthesis in developing skin in relation to innervation and expression of the receptor. *Nature 1987 326:6111*, *326*(6111), 353–358. https://doi.org/10.1038/326353a0

Diehn, M., Cho, R. W., Lobo, N. A., Kalisky, T., Dorie, M. J., Kulp, A. N., Qian, D., Lam, J. S., Ailles, L. E., Wong, M., Joshua, B., Kaplan, M. J., Wapnir, I., Dirbas, F. M., Somlo, G., Garberoglio, C., Paz, B., Shen, J., Lau, S. K., … Clarke, M. F. (2009). Association of Reactive Oxygen Species Levels and Radioresistance in Cancer Stem Cells. *Nature*, *458*(7239), 780. https://doi.org/10.1038/NATURE07733

Dongre, A., & Weinberg, R. A. (2018). New insights into the mechanisms of epithelial–mesenchymal transition and implications for cancer. *Nature Reviews Molecular Cell Biology 2018 20:2*, *20*(2), 69–84. https://doi.org/10.1038/s41580-018-0080-4

Elkashty, O. A., Elghanam, G. A., Su, X., Liu, Y., Chauvin, P. J., & Tran, S. D. (2020). Cancer stem cells enrichment with surface markers CD271 and CD44 in human head and neck squamous cell carcinomas. *Carcinogenesis*, *41*(4), 458–466. https://doi.org/10.1093/CARCIN/BGZ182

Frank, N. Y., Schatton, T., & Frank, M. H. (2010). The therapeutic promise of the cancer stem cell concept. *The Journal of Clinical Investigation*, *120*(1), 41–50. https://doi.org/10.1172/JCI41004

Im, K., Mareninov, S., Diaz, M. F. P., & Yong, W. H. (2019). An introduction to Performing Immunofluorescence Staining. *Methods in Molecular Biology (Clifton, N.J.)*, *1897*, 299. https://doi.org/10.1007/978-1-4939-8935-5_26

Joshua, B., Kaplan, M. J., Doweck, I., Pai, R., Weissman, I. L., Prince, M. E., & Ailles, L. E. (2012). Frequency of cells expressing CD44, a Head and Neck cancer stem cell marker: Correlation with tumor aggressiveness. *Head & Neck*, *34*(1), 42–49. https://doi.org/10.1002/HED.21699

Kalluri, R., & Weinberg, R. A. (2009). The basics of epithelial-mesenchymal transition. *The Journal of Clinical Investigation*, *119*(6), 1420–1428. https://doi.org/10.1172/JCI39104

Kapałczyńska, M., Kolenda, T., Przybyła, W., Zajączkowska, M., Teresiak, A., Filas, V., Ibbs, M., Bliźniak, R., Łuczewski, Ł., & Lamperska, K. (2018). 2D and 3D cell cultures – a comparison of different types of cancer cell cultures. *Archives of Medical Science : AMS*, *14*(4), 910. https://doi.org/10.5114/AOMS.2016.63743

Koenig, A., Wojcieszyn, J., Weeks, B. R., & Modiano, J. F. (2001). Expression of S100a, Vimentin, NSE, and Melan A/MART-1 in Seven Canine Melanoma Cell Lines and Twenty-nine Retrospective Cases of Canine Melanoma. *Veterinary Pathology*, *38*(4), 427–435. https://doi.org/10.1354/vp.38-4-427

Mani, S. A., Guo, W., Liao, M. J., Eaton, E. N., Ayyanan, A., Zhou, A. Y., Brooks, M., Reinhard, F., Zhang, C. C., Shipitsin, M., Campbell, L. L., Polyak, K., Brisken, C., Yang, J., & Weinberg, R. A. (2008). The Epithelial-Mesenchymal Transition Generates Cells with Properties of Stem Cells. *Cell*, *133*(4), 704–715. https://doi.org/10.1016/J.CELL.2008.03.027/ATTACHMENT/837EA262-762F-412E-9C02-032F2B4E0807/MMC1.PDF

Meacham, C. E., & Morrison, S. J. (2013). Tumour heterogeneity and cancer cell plasticity. *Nature 2013 501:7467*, *501*(7467), 328–337. https://doi.org/10.1038/nature12624

Morath, I., Hartmann, T. N., & Orian-Rousseau, V. (2016). CD44: More than a mere stem cell marker. *The International Journal of Biochemistry & Cell Biology*, *81*, 166–173. https://doi.org/10.1016/J.BIOCEL.2016.09.009

Murillo-Sauca, O., Chung, M. K., Shin, J. H., Karamboulas, C., Kwok, S., Jung, Y. H., Oakley, R., Tysome, J. R., Farnebo, L. O., Kaplan, M. J., Sirjani, D., Divi, V., Christopher Holsinger, F., Tomeh, C., Nichols, A., Le, Q. T., Dimitrios Colevas, A. A., Kong, C. S., Uppaluri, R., … Sunwoo, J. B. (2014). CD271 is a functional and targetable marker of tumor-initiating cells in head and neck squamous cell carcinoma. *Oncotarget*, *5*(16), 6854. https://doi.org/10.18632/ONCOTARGET.2269

Naor, D., Sionov, R. V., & Ish-Shalom, D. (1997). CD44: Structure, Function and Association with the Malignant Process. *Advances in Cancer Research*, *71*, 241–319. https://doi.org/10.1016/S0065-230X(08)60101-3

Ngo, M., Han, A., Lakatos, A., Sahoo, D., Hachey, S. J., Weiskopf, K., Beck, A. H., Weissman, I. L., & Boiko, A. D. (2016). Antibody Therapy Targeting CD47 and CD271 Effectively Suppresses Melanoma Metastasis in Patient-Derived Xenografts. *Cell Reports*, *16*(6), 1701–1716. https://doi.org/10.1016/J.CELREP.2016.07.004/ATTACHMENT/BC98692E-E747-46F6-803A-8092D83FDF36/MMC1.PDF

Nimmakayala, R. K., Batra, S. K., & Ponnusamy, M. P. (2019). Unraveling the journey of cancer stem cells from origin to metastasis. *Biochimica et Biophysica Acta. Reviews on Cancer*, *1871*(1), 50. https://doi.org/10.1016/J.BBCAN.2018.10.006

Oh, S. Y., Kang, H. J., Kim, Y. S., Kim, H., & Lim, Y. C. (2013). CD44-negative cells in head and neck squamous carcinoma also have stem-cell like traits. *European Journal of Cancer*, *49*(1), 272–280. https://doi.org/10.1016/J.EJCA.2012.06.004/ATTACHMENT/B9B3D9C0-B7FD-4AF0-9182-BF54D4D3FFB3/MMC3.PPTX

Pei, D., Shu, X., Gassama-Diagne, A., & Thiery, J. P. (2019). Mesenchymal–epithelial transition in development and reprogramming. *Nature Cell Biology 2019 21:1*, *21*(1), 44–53. https://doi.org/10.1038/s41556-018-0195-z

Quintana, E., Shackleton, M., Sabel, M. S., Fullen, D. R., Johnson, T. M., & Morrison, S. J. (2008). Efficient tumour formation by single human melanoma cells. *Nature 2008 456:7222*, *456*(7222), 593–598. https://doi.org/10.1038/nature07567

Radke, J., Roßner, F., & Redmer, T. (2017). CD271 determines migratory properties of melanoma cells. *Scientific Reports*, *7*(1). https://doi.org/10.1038/S41598-017-10129-Z

Reya, T., Morrison, S. J., Clarke, M. F., & Weissman, I. L. (2001). Stem cells, cancer, and cancer stem cells. *Nature 2001 414:6859*, *414*(6859), 105–111. https://doi.org/10.1038/35102167

Rosen, R. D., & Sapra, A. (2022). TNM Classification. *StatPearls NCBI*. https://www.ncbi.nlm.nih.gov/books/NBK553187/

Saltari, A., Truzzi, F., Quadri, M., Lotti, R., Palazzo, E., Grisendi, G., Tiso, N., Marconi, A., & Pincelli, C. (2016). CD271 Down-Regulation Promotes Melanoma Progression and Invasion in Three-Dimensional Models and in Zebrafish. *Journal of Investigative Dermatology*, *136*(10), 2049–2058. https://doi.org/10.1016/J.JID.2016.05.116

Schmid, F., Brodesser, D., Reifinger, M., Forte, S., Semp, P., Eberspächer-Schweda, M. C., Wolschek, M., Brandt, S., Kleiter, M., & Pratscher, B. (2019). Canine oral primary melanoma cells exhibit shift to mesenchymal phenotype and phagocytic behaviour. *Veterinary and Comparative Oncology*, *17*(3), 211–220. https://doi.org/10.1111/VCO.12464

Segeritz, C. P., & Vallier, L. (2017). Cell Culture: Growing Cells as Model Systems In Vitro. *Basic Science Methods for Clinical Researchers*, 151–172. https://doi.org/10.1016/B978-0-12-803077-6.00009-6

Strohmayer, C., Klang, A., Kummer, S., Walter, I., Jindra, C., Weissenbacher-Lang, C., Redmer, T., Kneissl, S., & Brandt, S. (2022). *Tumor Cell Plasticity in Equine Papillomavirus-Positive Versus-Negative Squamous Cell Carcinoma of the Head and Neck*. https://doi.org/10.3390/pathogens11020266

Thankamony, A. P., Saxena, K., Murali, R., Jolly, M. K., & Nair, R. (2020). Cancer Stem Cell Plasticity – A Deadly Deal. *Frontiers in Molecular Biosciences*, *7*, 79. https://doi.org/10.3389/FMOLB.2020.00079/BIBTEX

Vitale, I., Manic, G., de Maria, R., Kroemer, G., & Galluzzi, L. (2017). DNA Damage in Stem Cells. *Molecular Cell*, *66*(3), 306–319. https://doi.org/10.1016/J.MOLCEL.2017.04.006

Yan, Y., Zuo, X., & Wei, D. (2015). Concise Review: Emerging Role of CD44 in Cancer Stem Cells: A Promising Biomarker and Therapeutic Target. *Stem Cells Translational Medicine*, *4*(9), 1033–1043. https://doi.org/10.5966/SCTM.2015-0048

Yang, J., & Weinberg, R. A. (2008). Epithelial-Mesenchymal Transition: At the Crossroads of Development and Tumor Metastasis. *Developmental Cell*, *14*(6), 818–829. https://doi.org/10.1016/J.DEVCEL.2008.05.009

Yoder, M. C. (2004). Biology of Stem Cells and Stem Cell Transplantation. *Fetal and Neonatal Physiology: Third Edition*, *2–2*, 1365–1373. https://doi.org/10.1016/B978-0-7216-9654-6.50146-6

8. Appendices

8.1. List of Abbreviations

Canine oral malignant melanoma	cOMM
Human malignant melanoma	hMM
Multi drug resistance	MDR
Epithelial-mesenchymal transition	EMT
Mesenchymal-epithelial transition	MET
Cancer stem cells	CSC
Cluster of differentiation	CD
Extracellular matrix	ECM
Two-Dimensional	2D
Three-Dimensional	3D
Immunofluorescence	IF
Immunohistochemistry	IHC
Immunocytochemistry	ICC
Antibody	AB
Flow cytometry	FC
Fluorescent-activated cell sorting	FACS
Dulbecco's Modified Eagle's Medium + GlutaMAX™	DMEM
Foetal calf serum	FCS
Complete medium	CM
Dulbecco's Phosphate Buffer Saline	DPBS
4',6-diamidino-2-phenylindole	DAPI
Live/Death	L/D
Haematoxylin/Eosin	H/E
No primary control	NPC

8.2. List of Figures

8.3. List of Tables